Available online at www.sciencedirect.com
ScienceDirect
European Journal of Pharmaceutics and Biopharmaceutics 64 (2006) 360–368
European Journal of Pharmaceutics and Biopharmaceutics
www.elsevier.com/locate/ejpb

Research paper

Preparation and in vitro/in vivo evaluation of nano-sized crystals for dissolution rate enhancement of ucb-35440-3, a highly dosed poorly water-soluble weak base

J. Hecq [a], M. Deleers [b], D. Fanara [b], H. Vranckx [b], P. Boulanger [c], S. Le Lamer [c], K. Amighi [a,*]

[a] *Laboratory of Pharmaceutics and Biopharmaceutics, Université Libre de Bruxelles, Campus Plaine, Boulevard du Triomphe, Brussels, Belgium*
[b] *UCB S.A., Department of Product Process and Analytical Developments, Chemin du Foriest, Braine-l'Alleud, Belgium*
[c] *UCB S.A., R&D, Laboratory of Drug Metabolism and Pharmacokinetics, Chemin du Foriest, Braine-l'Alleud, Belgium*

Received 15 March 2006; accepted in revised form 18 May 2006
Available online 18 July 2006

Abstract

ucb-35440-3 is a new drug entity under investigation at UCB S.A. Due to its physicochemical characteristics, the drug, a poorly water-soluble weak base, shows poor solubility and dissolution characteristics. In rat, the low oral bioavailability ($F < 10\%$) is largely due to poor absorption. In order to enhance the solubility and dissolution characteristics, formulation of ucb-35440-3 as nanocrystals has been achieved in this study. Nanoparticles were prepared using high pressure homogenization and were characterized in terms of size and morphology. In vitro dissolution characteristics were investigated and compared to the un-milled drug in order to verify the theoretical hypothesis on the benefit of increased surface area. In vivo pharmacokinetic evaluation of ucb-35440-3 nanoparticles was also carried out on rats. Crystalline state evaluation before and following particle size reduction was conducted through polarized light microscopy and PXRD to denote any possible transformation to an amorphous state during the homogenization process. Drug chemical stability was also assessed following homogenization. The dissolution rate increased significantly at pH 3.0, 5.0 and 6.5 for ucb-35440-3 nanoparticles. However, the pharmacokinetic profile obtained yielded lower systemic exposure than the un-milled compound (in fed state), this although being thought to be the consequence of the drug and formulation characteristics.

Keywords: Nanoparticles; High pressure homogenization; Dissolution; Drug reprecipitation; In vivo evaluation

1. Introduction

Poor aqueous solubility is actually a very challenging problem in drug formulation development as it is considered, at least for BCS class II compounds, to be, in association to poor dissolution characteristics, the limiting step to drug absorption from the gastrointestinal tract [1], in association to poor dissolution characteristics. As an increasing number of newly developed drug entities present such characteristics, approaches to overcome this factor are of great importance.

Among the various solubility/dissolution rate enhancement methodologies available for poorly water-soluble compounds (e.g. amorphous dispersions as solid dispersions/inclusion complexes, salt formation, surfactant/lipid based excipients addition, etc.), drug particle size reduction is meeting great interest in drug formulation [2,3]. Size reduction offers, in regard to the Noyes–Whitney and Ostwald–Freundlich equations, increased dissolution and solubility characteristics. Size reduction to nanometer

* Corresponding author. Laboratory of Pharmaceutics and Biopharmaceutics, Université Libre de Bruxelles, Campus Plaine, CP 207, Boulevard du Triomphe, 1050 Brussels, Belgium. Tel.: +32 2 650 5254; fax: +32 2 650 5269.
E-mail address: k.amighi@ulb.ac.be (K. Amighi).

0939-6411/$ - see front matter © 2006 Elsevier B.V. All rights reserved.
doi:10.1016/j.ejpb.2006.05.008

range has been shown to be a very promising approach as it increases specific surface area further than micronization and thus leads to enhanced dissolution characteristics and increased systemic exposure (for BCS class II compounds). Nanoparticles have been showed in various in vivo studies to significantly enhance oral bioavailability of poorly water-soluble drugs [4,5]. ucb-35440-3 nanoparticles were obtained through high pressure homogenization. This milling technique has been extensively described by Müller and co-workers [6–9].

ucb-35440-3 (Patent No. WO 00/58295), a new drug entity under investigation at UCB S.A. for the oral treatment of asthma and allergic rhinitis, was used as a model drug. The molecule, a poorly water soluble weak base (fumarate salt), presents two ionisable ternary nitrogen placed in a piperazine cycle ($pK_a \approx 9.6$; 5.7) (Fig. 1). Given the interesting results obtained in recent work with nifedipine nanoparticles [10], evaluation of the size reduction technology on ucb-35440-3 was carried out. ucb-35440-3 shows interesting features study-wise as, when compared to nifedipine, it is a highly dosed drug (anticipated human pharmacologically active dose should have been predicted at around 250–500 mg/day) and that it shows a pH-dependant solubility profile.

The object of this paper was to evaluate high pressure homogenization on the efficiency of ucb-35440-3 particle size reduction to nanometer range and to evaluate the hypothesis of enhanced dissolution properties at this size range. Correlation of the in vitro dissolution results with the pharmacokinetic profile following oral administration in rats was also evaluated. Drug crystalline state and chemical stability was also assessed to denote any possible alteration during the milling operation.

2. Materials and methods

2.1. Materials

ucb-35440-3 was supplied from UCB S.A.. Methocel E15 (hydroxy-propylmethylcellulose – HPMC) and Methocel A400 (methylcellulose – MC) were purchased from Colorcon (West Point, PA, USA). Polyvinyl alcohol (M_W 13,000–23,000) was purchased from Aldrich Chemical Company Inc. (Milwaukee, WIS, USA). Texapon K 12® (sodium dodecyl sulfate) was purchased from Henkel (Düsseldorf, Germany). Acacia gum was purchased from Sigma–Aldrich (St. Louis, MO, USA). Lutrol F127® (equivalent to poloxamer 407) was purchased from BASF (Ludwigsbafen, Germany). Water was obtained using a CFOF 01205 Milli-Q Water Purification System (Millipore Corporation, Bedford, MA, USA). All other materials were of analytical reagent grade.

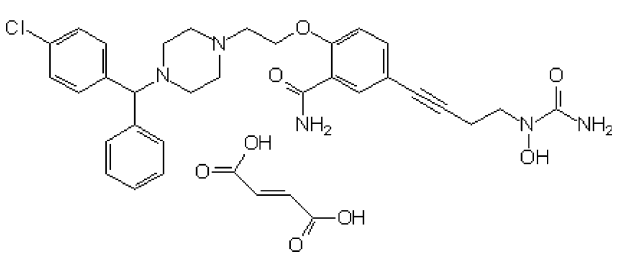

Fig. 1. Chemical structure of ucb-35440-3 (5-{4-[(aminocarbonyl)-(hydroxy)amino]but-1-ynyl}-2-(2-{4-[(*R*)-(4-chlorophenyl)(phenyl)methyl]-piperazin-1-yl}ethoxy)benzamide).

2.2. Preparation of samples

The steps in the preparation of drug nanoparticles were as follows.

2.2.1. Preparation of drug nanosuspensions

ucb-35440-3 powder was poured in an aqueous surfactant solution (5% ucb-35440-3 w/v suspensions) (all surfactants tested were used at a concentration of 2% w/w relative to ucb-35440-3 content) under magnetic stirring (500 rpm). Nanosuspensions were prepared using an EmulsiFlex-C5 high pressure homogenizer (HPH) (Avestin Inc., Ottawa, Canada). Pre-milling low-pressure homogenization cycles (C) were run before the high pressure homogenizing cycles for a first significant size reduction (preventing blockage of the homogenizing gaps which present relatively low openings at the high pressure used; i.e. ±25 μm at 22,000 psi ([7]). The pre-milling low pressure cycles adopted are 15 cycles at 7000 psi and 10 cycles at 12,000 psi. High pressure homogenization was then finally applied for 10–20 cycles at 23–24,000 psi. During all pre-milling and milling cycles, agitation (Ultra-Turrax® T25 Basic – 8000 rpm, IKA®-Werke GmbH & Co. KG, Staufen, Germany) was maintained in the sample reservoir to avoid sedimentation of particles. As ucb-35440-3 is heat-sensitive and the HPH causes sample temperature increase (increase of 30 °C following 20 °C at 24,000 psi), all operations were carried out using an heat exchanger, placed ahead of the homogenizing valve, with sample temperature maintained at 10 ± 1 °C. Samples were withdrawn after the different size-reduction steps for size distribution analysis.

2.2.2. Water-removal

In order to retrieve nanoparticles in dried-powder state from the nanosuspensions, water-removal was conducted through freeze-drying. The homogenized suspensions were frozen at −80 °C overnight and freeze-dried using a Lyovac GT-2 apparatus (Leybold–Heraeus, Köln, Germany) under vacuum (pressure < 0.01 mbar) for 15 h in open Petri dishes.

2.3. Particle size and shape characterization

Size and size distribution of the particles in suspension following the different homogenization steps and in dried-state following water redispersion were determined through laser diffraction (LD), with a wet-sampling

system (MasterSizer 2000, Malvern Instruments, Worcestershire, UK). The diameters reported were calculated using volume distribution. The median-volume particle size, $d(v, 0.5)$ (size of the particles for which 50% of the sample volume contains particles smaller than 'd 0.5', the other particles being larger than 'd 0.5'), $d(v, 0.1)$, $d(v, 0.9)$ and the volume mean diameter $D[4,3]$ were used as characterization parameters. The refractive and absorption indexes of ucb-35440-3 were both approximated, by selection of the combination yielding the best residuals and fit data, at 1.610 and 0.001, respectively, and were used for measurements conducted. Morphological evaluation of nanoparticles was conducted through scanning electron microscopy (SEM) (JSM-6100, JEOL, Tokyo, Japan) following platinum coating.

2.4. Dissolution – solubility

A Distek 2100C USP dissolution apparatus (Distek Inc., North Brunswick, NJ, USA) Type II (paddle method) operating at a rotation speed of 60 rpm was used for in vitro testing of drug dissolution. All dissolution tests were carried out on an equivalent of 200 mg of ucb-35440-3 (in powder state) placed into HPMC capsules (placed into sinkers). Fifty millimoles phosphate buffers (0.05% polysorbate 20) at pH 3.0, 5.0 and 6.5 were used as dissolution media. The volume and temperature of the dissolution medium were 900 ml and 37.0 ± 0.2 °C respectively. Automatic withdrawals at fixed times were filtered in-line and assayed through ultraviolet absorbance determination at 255 nm using an Agilent 8453 UV/visible Dissolution Testing System (Agilent Technologies, USA). The mean results of triplicate measurements and the standard deviation were reported. Saturation solubility evaluations were carried out at varying pHs at 25 °C following shaking of 10 mg/ml suspensions for 70 h (saturation checked). Withdrawals were filtered on 0.45 μm pore membranes. A Kontron chromatograph HPLC system type 400 (Kontron Instruments, Eching, Germany) was used for ucb-35440-3 quantification. Chromatographic separation was accomplished using a Kromasil C18, 3.5 μm, 250×4.6 mm stainless steel column (AIT Chromato, France). The mobile phase consisted of a solvent A (ACN 10%/phosphate buffer, pH 3.0 90%)/solvent B (ACN 75%/phosphate buffer, pH 3.0 25%) mixture (50:50 v/v). The mobile phase was pumped isocratically at a flow rate of 1.0 ml/min during analysis, at 25 °C. The effluent was monitored at 210 nm.

2.5. Crystalline state evaluation of dried samples

2.5.1. Powder X-ray diffraction (PXRD)

PXRD diffractograms were recorded using a Siemens D5000 diffractometer (Siemens, Germany) with a Cu line as the source of radiation. Standard runs using a 40 kV voltage, a 40 mA current and a scanning rate of 0.02°/min over a 2θ range of 2–40° were used.

2.5.2. Polarized light microscopy

Optical microscopy analysis was conducted on an Olympus-BX 60 microscope (Olympus – Nihon Koden, Japan) equipped with a JVC TK-C1381 colour video camera (JVC, Japan). A U-POT Polaroid filter is placed ahead of the sample for light polarization.

2.6. In vivo PK study

2.6.1. Animals

Male Wistar rats (6–7 weeks old) were obtained from Charles River Laboratories (Charles River, Brussels, Belgium). The rats' weights ranged from 180 to 200 g. All animals had free access to tap water and pelleted diet. Fasted rats were deprived of food 18 h before the experiment and food was reoffered 4 h post-dosing. ucb-35440-3 suspensions were administered orally to six male Wistar rats at a dose of 100 mg/kg. Suspensions of un-milled drug and drug nanoparticles (un-buffered suspension/0.5 M phosphate, pH 6.5, buffered suspension) were dosed at 10 ml/kg. For homogeneity reasons, un-milled ucb-35440-3 suspensions were prepared in 1% Methocel A400 solutions (i.e. particle sedimentation). Six hundred microliters blood samples were withdrawn from the caudal vein at predose, 30 min, 1, 2, 4, 8, 12 and 24 h post-dosing and placed into Li Heparin plastic tubes. Blood samples were held on ice (+4 °C) until centrifuged at 3000g, 4 °C for 5 min. Plasma was transferred to individual Eppendorfs and stored at −20 °C until analysed.

2.6.2. Analysis

2.6.2.1. Sample preparation procedure. Plasma samples were prepared by liquid–liquid extraction. Two hundred microliters of plasma sample were pipetted into an Eppendorf tube and fortified with 50 μL of the internal standard (ucb-46680) working solution (100 ng/mL). Three hundred microliters of a glycine–sodium chloride 2.0 mol/L buffer adjusted at pH 10.0 with sodium hydroxide 2.0 mol/L were added. The content of the tube was gently mixed and then extracted with 1 mL of hexane–isopropanol 1:1 (v/v). This involved thorough vortex-mixing for 10 min and subsequent centrifugation at 13,000 rpm (H 14750g) for 10 min. The upper organic phase was transferred into another Eppendorf tube and evaporated to dryness in a preheated concentrator–evaporator (pulse vent = 1, heating level = 0) (JOUAN RC 10.22; Saint-Herblain, France). The residue was reconstructed with 75 μL of acetonitrile–water 23:77 (v:v) containing 0.1% trifluoroacetic acid and adjusted to pH 3.0 with ammonium hydroxide, vortex mixed and then filtered on a Ultrafree MC 0.45 μm device at 13,000 rpm (H 14750g) for 15 min using an ALC microcentrifuge 4214 (Milan, Italy). An aliquot (10 μL) was injected into the LC/ESI/MS/MS system described below.

2.6.2.2. ucb-35440-3 analysis. A HP1100 HPLC system (Hewlett–Packard, Palo Alto, USA), coupled to a Quattro Ultima mass spectrometer (Micromass, Manchester, UK)

was used to measure ucb-35440-3 in plasma samples. The analytical column (Inertsil ODS 3, 5 μm, 50 × 2.1 mm ID (Varian, Harbor City, USA)) was protected by a guard column (Inertsil ODS 3, 5 μm, 10 × 2.1 mm ID (Varian, Harbor City, USA)). The column and the pre-column were placed in an oven set to a temperature of 40 °C. Analyses were performed in a binary gradient mode. Solvents A and B consisted of acetonitrile–water 5:95 and 95:5 (v/v), respectively, both containing 0.1% trifluoroacetic acid and adjusted to pH 3.0 with ammonium hydroxide. The HPLC gradient started at 25% B and was linearly increased to 50% B over 7 min. It was then increased to 100% B over 0.1 min (0.9 min hold) before returning to 25% B over 0.1 min. The system was allowed to re-equilibrate for 1.9 min before injection of the next sample. The flow was adjusted to 0.250 mL/min and split post-column (ratio of 1:5) in order to get 0.050 mL/min into the electrospray source. Electrospray experiments used a capillary voltage set at 4.00 kV. The source temperature was kept at 100 °C and the desolvation temperature at 350 °C. The cone gas flow (N_2) was adjusted to *ca* 90 L/h and the desolvation gas flow (N_2) to *ca* 850 L/h. The collision gas pressure (argon) was adjusted to about 2×10^{-3} mbar. Spectra were acquired at *ca*. 1 mass unit resolution (10% valley definition) for parent and daughter ions. The inter-channel delay was fixed at 0.1 s. ucb-35440-3 concentrations were determined by the peak area ratio technique. The limit of quantification of the method is 0.5 ng/ml. Calibration curves were established over a range of 0.5–100 ng/ml ($r^2 > 0.997$) and study samples were diluted with blank human plasma when required.

2.6.2.3. Data processing. Individual plasma concentrations and nominal sampling times were used to assess the pharmacokinetic parameters by non-compartmental analysis using the Watson Lims (6.4.0.03, Innaphase, Philadelphia, PA, USA). C_{max} refers to the peak plasma level and t_{max} refers to the time at which C_{max} occurred. The area under the curve AUC$(0 - t)$ (i.e. area under the concentration–time curve calculated from zero up to time corresponding to the last measurable concentration) was calculated using the linear trapezoidal rule using individual concentrations.

3. Results and discussion

3.1. Nanoparticle preparation

Un-milled ucb-35440-3 used in this study was characterized by relatively large particles ($d(v, 0.5)$ about 140 μm as reported in Fig. 2 and particles up to 500 μm). These particles had to follow preliminary size-reduction steps prior to the high pressure homogenization operation in order to be small enough to pass the homogenizing gaps of the homogenizer at the homogenizing pressures used (i.e. 25 μm at 22,000 psi [7]. Fig. 2 shows that low pressure pre-milling homogenizing cycles were found to be very effective as preliminary size reduction step when compared to previous work with another model drug where similar cycles were used [10], as a population with $d(v; 0.5)$ of around 600 nm and comprising 59% (in volume) of sub-micron particles is obtained. The following high pressure homogenization cycles were shown to further decrease particle size; the size distribution being characterized by $d(v, 0.5)$ of around 200 nm and comprising 83% (in volume) of sub-micron particles. Additional high pressure homogenization cycles (up to 20) were found to slightly decrease only $d(v, 0.9)$ and $D[4,3]$ with $d(v, 0.5)$ and $d(v, 0.1)$ being unaffected.

HPMC of low viscosity grade was chosen, at a concentration of 2% w/w relative to ucb-35440-3 content, for

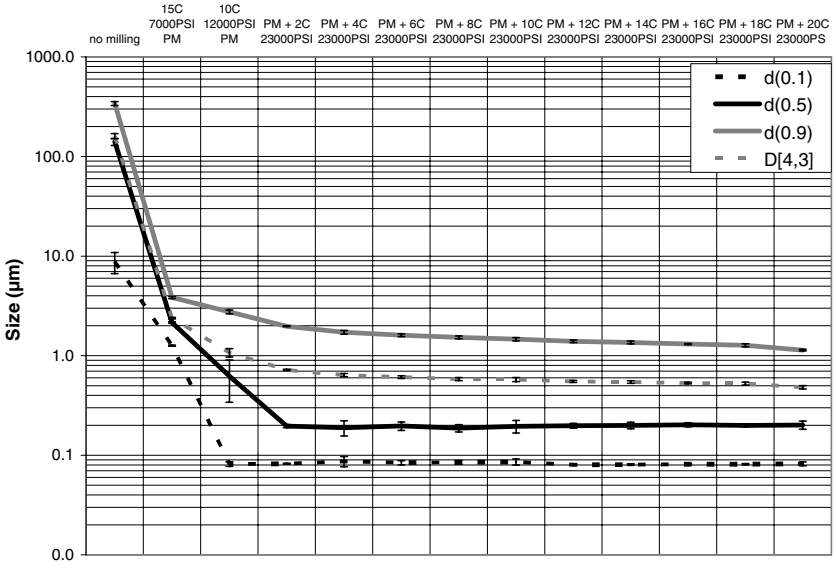

Fig. 2. Influence of pre-milling (PM) operation and number of high pressure homogenization cycles (C) on ucb-35440-3 particle size for a ucb-35440-3 5% – HPMC 0.1% w/w suspension.

Table 1
Surfactant screening (% w/w relative to ucb-35440-3 content) – particle size ($n \geqslant 10$: mean ± SD) following PMC + 10C 23,000 psi

		$d(v, 0.5) \pm$ SD (μm)	$d(v, 0.1) \pm$ SD (μm)	$d(v, 0.9) \pm$ SD (μm)	$D[4,3] \pm$ SD (μm)
Sodium lauryl sulfate	2%	10.7 ± 1.9	5.42 ± 1.02	20.3 ± 3.7	11.9 ± 2.1
HPMC (Methocel E15)	2%	0.182 ± 0.007	0.083 ± 0.001	1.46 ± 0.05	0.563 ± 0.023
Polyvinyl alcohol	2%	0.262 ± 0.054	0.082 ± 0.002	1.50 ± 0.10	0.603 ± 0.038
Acaciae Gum	2%	0.407 ± 0.006	0.090 ± 0.001	1.18 ± 0.05	0.542 ± 0.016
Poloxamer 407	2%	0.183 ± 0.003	0.079 ± 0.001	1.20 ± 0.05	0.483 ± 0.011

nanosuspension stabilization. This was because this water-soluble polymer offers adequate surface active properties (i.e. stabilization of nanoparticles formed during homogenization) when compared to other commonly used surfactants such as sodium dodecyl sulfate, polyvinyl alcohol and acacia gum (Table 1), and because it is a widely used pharmaceutical excipient with no known toxicity. Although poloxamers have been shown to be quite successful in regard to nanoparticle stabilization, their use is limited due to their low melting-point characteristics which are problematic for further sample processing (i.e. freeze-drying and especially spray-drying operations). As observed in previous studies when no carriers (i.e. mannitol) are used [10] and on the SEM micrograph of Fig. 3, nanoparticle agglomeration is clearly observed following water-removal from the nanosuspensions (redispersion of the freeze-dried powder, yielding a population with $d(v, 0.5)$ around 90 μm and no submicron particles). Although the presence of a carrier is very useful regarding optimization of nanoparticle redispersion characteristics following water-removal, none was used in this study; the projected ucb-35440-3 dose being set at 200 mg, further addition of excipients for sample processing was limited due to the low density of the powder obtained.

3.2. Dissolution rate evaluation

Being a weak base, ucb-35440-3 presents a pH-dependant solubility profile; solubility decreasing with increasing pH (Fig. 4) and being predictive of intestinal-dissolution and/or absorption limitations. According to this profile, dissolution evaluations were carried out at pH 3.0 (Aq. Sol. ~0.65 mg/ml), pH 5.0 (Aq. Sol. ~0.2 mg/ml) and pH 6.5 (Aq. Sol. < 0.03 mg/ml). Dissolution profiles at these pHs, with comparison of un-milled ucb-35440-3 and ucb-35440-3 nanoparticles, are respectively shown in Fig. 5A–C. The approximate 10 min lag time observed for each formulation can be attributed to capsule disintegration. Dissolution rate (DR) enhancement is clearly observed at all tested pHs. At pH 3.0, more than 95% of the drug was already dissolved after 60 min for ucb-35440-3 nanoparticles compared to dissolution of around 30% of the un-milled ucb-35440-3 after the same time period and complete dissolution being unachieved for the latest over a span of 13 h. Similar observations could be made for dissolution at pH 5.0 (which is less favorable to ucb-35440-3 dissolution) as after 60 min, 85% of the drug in nanoparticle form was already dissolved compared to 20% of un-milled ucb-35440-3, with the same observation regarding complete dissolution as for pH 3.0. Increased DR for ucb-35440-3 nanoparticles was also observed at pH 6.5 (Fig. 5C), where after 60 min approximately 20% of the drug was dissolved compared to 3% for un-milled ucb-35440-3. Due to the low saturation solubility, saturation of the dissolution media is rapidly reached for nanoparticles at this pH, and recrystalization is observed. Drug dissolution at this pH shall be evaluated under different conditions (e.g. flow-through dissolution). Standard deviations observed in the dissolution profiles were also shown to be smaller for ucb-35440-3 nanoparticles; un-milled drug received as a coarse powder with a large polydispersity.

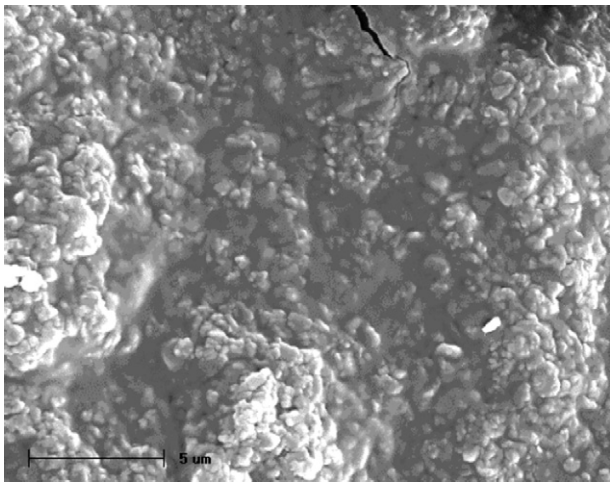

Fig. 3. SEM micrograph of a freeze-dried ucb-35440-3 nanosuspension (magnification 5000×; scale = 5 μm).

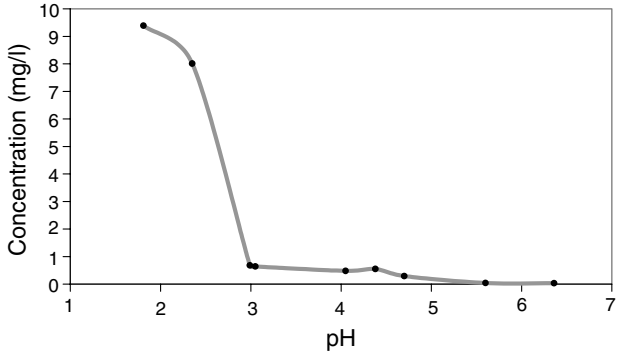

Fig. 4. Aqueous solubility profile (25 °C) of un-milled ucb-35440-3.

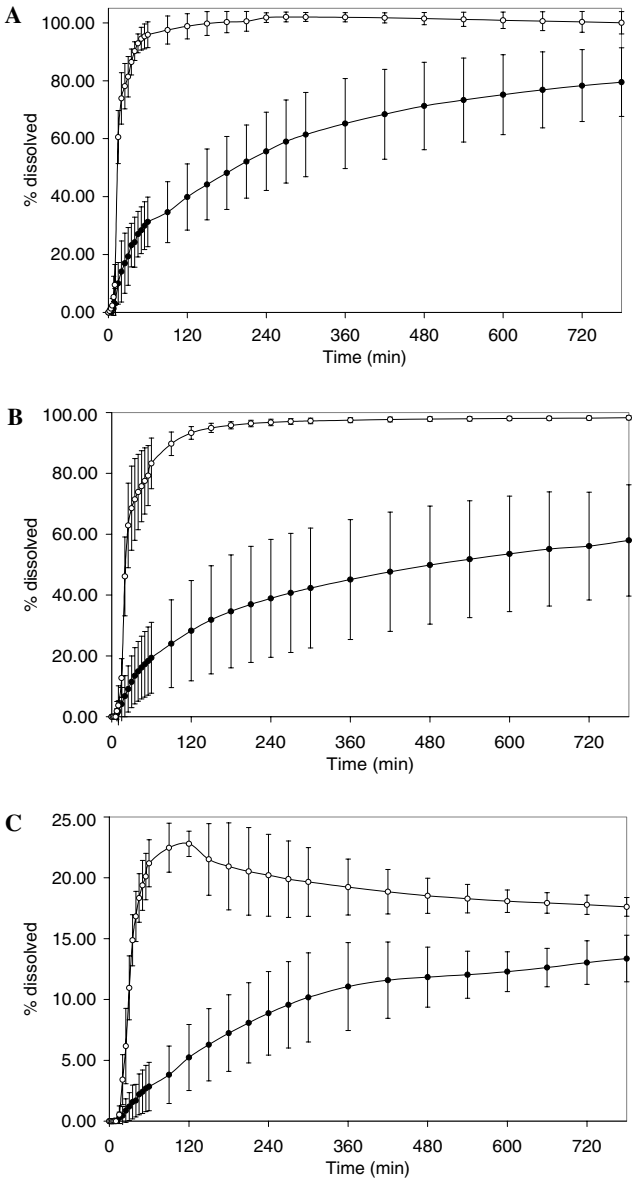

Fig. 5. Dissolution profiles [phosphate 50 mM buffer, pH 3.0 (A); 5.0 (B) and 6.5 (C)] for un-milled ucb-35440-3 (●) and for ucb-35440-3 5% – HPMC 0.1% freeze-dried nanosuspensions (○) samples (mean ± SD – $n \geqslant 3$).

3.3. Crystalline state evaluation

To verify that the DR increase observed for ucb-35440-3 nanoparticles is not the consequence of the presence of amorphous drug (the un-milled drug received in crystalline powder form), crystalline state evaluation was carried out after the homogenization operation. Polarized-light optical microscopy analysis clearly showed the anisotropic nature of the un-milled drug (Fig. 6). The same observations can be made for ucb-35440-3 nanoparticles, indicating that crystalline state seems to be unaltered following the homogenization operation. PXRD diffractograms of Fig. 7 confirm this statement as the diffraction pattern is preserved for ucb-35440-3 nanoparticles. The decrease in peak intensity for certain diffraction angles can be attributed to the presence of HPMC at the surface of the particles, as it has already been reported in previous studies [10]. Chemical stability was also verified following high pressure homogenization as no degradation was observed (data not shown).

3.4. In vivo pharmacokinetic evaluation

Pharmacokinetic evaluation following an oral dose of 100 mg/kg (suspension state) of both ucb-35440-3 un-milled drug and nanoparticles was carried out on male Wistar rats in fed and fasted states. A positive food effect on the drug absorption is reported for the drug. Based on the pH-dependent solubility profile of the drug and as it is clearly shown when mimicking GIT pH conditions through in vitro dissolution tests (Fig. 8), reprecipitation entering small intestine should be expected. Fig. 8 shows the difference between the two ucb-35440-3 systems regarding dissolution at pH 1.3. It shows that the fast dissolution behaviour at this pH for the nanoparticulate formulation should allow for rapid drug disposal in the stomach (particularly if the stomach residence time is prolonged as it is the case in fed state). The data also suggest that when drug dissolution is so important at acidic pH, reprecipitation will occur when pH increases. LD analysis of the dissolution media after passage from pH 5.0 to 6.3, where most of the reprecipitation occurs, show a population of particles with a $d(v,0.5)$ of 2.68 ± 0.13 μm and no submicron particles. We can anticipate that this phenomenon might also be observed in vivo when entering small intestine. No data regarding the particles in the precipitate were retrieved, except for particle size; the physicochemical state of the drug in the precipitate being unknown.

To investigate the eventuality of drug reprecipitation following stomach exiting, as well as its consequence on drug absorption, formulation of ucb-35440-3 nanoparticles in a 0.5 M pH 6.5 phosphate buffer was assayed. This formulation was expected to limit drug dissolution in stomach and thus prevent the presumed drug reprecipitation following its exit. This limitation shall particularly be observed in fasted conditions where the stomach's pH is at its lowest (e.g. the rat stomach pH in fasted state and fed state being of 3 and 5, respectively [11]).

Fig. 9 shows the pharmacokinetic profile for un-milled ucb-35440-3 and for nanoparticle formulations in fed and fasted state. The results showed on Fig. 9 and Table 2 clearly indicate a positive food effect on ucb-35440-3 absorption. An extent of exposure of 7100 ng h/ml was found for fed animals compared to 327 ng h/ml for fasted animals (un-milled drug). The same conclusions could be drawn for ucb-35440-3 nanoparticles as an extent of exposure of 3736 and 2614 ng h/ml were found for fed animals compared to 1282 and 1366 ng h/ml for fasted animals, in un-buffered and buffered conditions, respectively.

When comparing the PK profile of the un-milled ucb-35440-3 formulation and the ucb-35440-3 nanoparticle

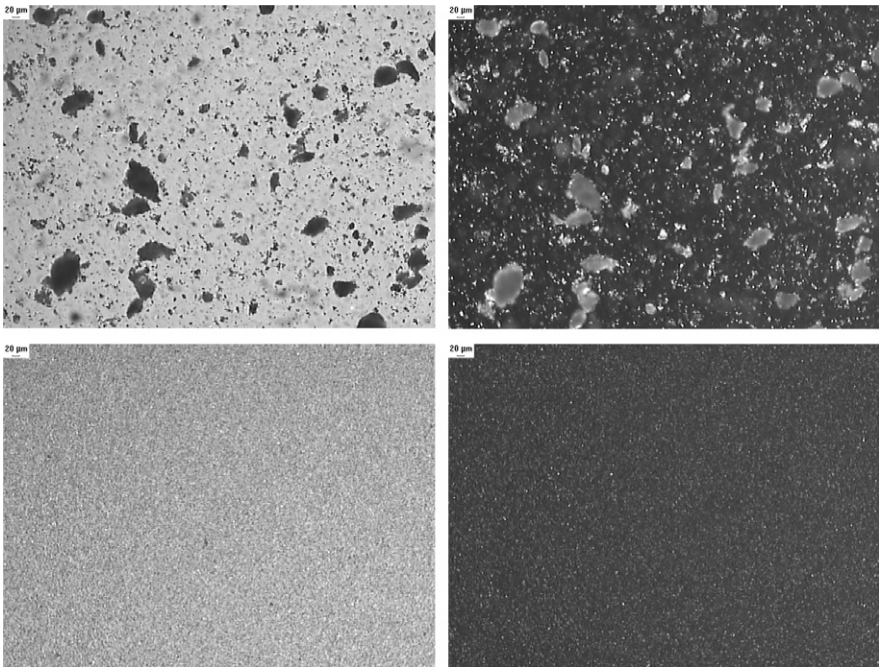

Fig. 6. Optical microscopy – polarized light (PL) analysis (magnification 50× – scale = 20 μm): un-milled ucb-35440-3 non PL (upper left) and PL (upper right); ucb-35440-3 nanosuspension non PL (lower left) and PL (lower right).

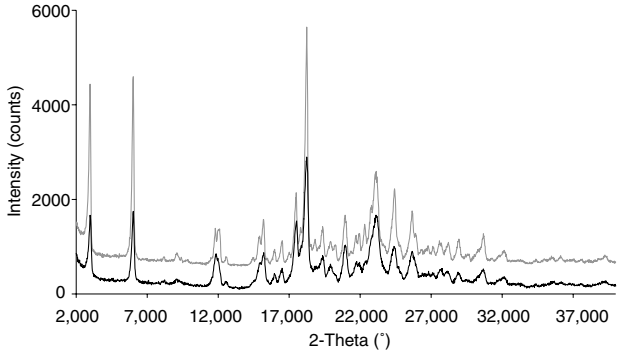

Fig. 7. PXRD diffractograms for un-milled ucb-35440-3 (gray) and ucb-35440-3 5% – HPMC 0.1% freeze-dried nanosuspension (black).

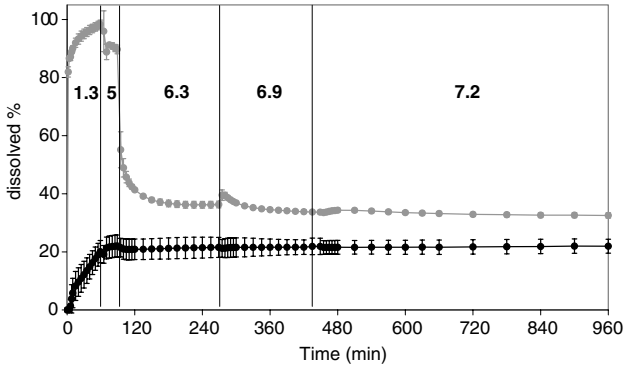

Fig. 8. Dissolution profiles (GIT pH simulation – 1.3 (1 h); 5 (0.5 h); 6.3 (3 h), 6.9 (3 h) and 7.2 (till end of test)) for un-milled ucb-35440-3 (●) and for ucb-35440-3 5% – HPMC 0.1% freeze-dried nanosuspension (●) samples (mean ± SD – $n = 3$).

formulations in both fed and fasted state, we observe, respectively, a decrease and an increase of the drug extent of exposure for ucb-35440-3 nanoparticles. Keeping in

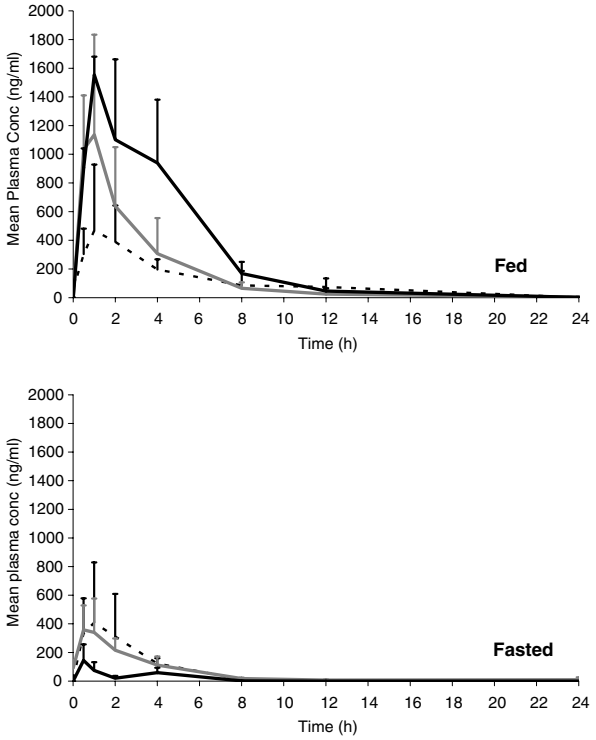

Fig. 9. Mean plasma concentrations (±SD) (fed state (top) and fasted state (bottom)) for un-milled ucb-35440-3 (Black bold line) (fed and fasted: $n = 3$); ucb-35440-3 nanoparticles (un-buffered suspension) (grey thick line) (fed and fasted: $n = 6$) and ucb-35440-3 nanoparticles (buffered suspension) (black dashed line) (fed: $n = 6$ and fasted: $n = 5$).

Table 2
Mean plasma pharmacokinetic parameter values for ucb-35440-3 in the Wistar rat after single oral administration (100 mg/kg) of different tested ucb-35440-3 formulations: influence of particle size and media buffering

	Fed			Fasted		
	C_{max} (ng/ml)	T_{max} (h)	Mean $AUC_{(0-t)}$ (ng h/ml)	C_{max} (ng/ml)	T_{max} (h)	Mean $AUC_{(0-t)}$ (ng h/ml)
Un-milled	1554 ± 127	1	7100	144 ± 112	0.5	327
Nano (un-buffered suspension)	1244 ± 594	0.75	3736	383 ± 202	0.75	1282
Nano (buffered suspension)	555 ± 396	1	2614	443 ± s390	0.5	1366

mind the pH dependant solubility profile of the drug, these observations can be explained by the amount of drug dissolved in the stomach and by the time given for this dissolution. The gastric residence time (GRT) being longer in fed state than in fasted state, the amount of dissolved ucb-35440-3 will be lower for the latest condition, this even though gastric pH is lower.

When comparing the three formulations in fasted state, where GRT is short and where only dissolution rate shall limit the amount of drug dissolved, we can clearly understand the increased extent of exposure for ucb-35440-3 nanosuspensions. No differences were observed between the buffered and un-buffered nanosuspension in fasted state. This could be explained by the fact that the amount of drug dissolved in the stomach for the un-buffered suspension might be higher than for the buffered suspension, but that drug reprecipitation might take place following stomach's exiting. Intestinal drug concentrations would thus be similar for the two suspensions. This observation could also find an explanation in the fact that gastric emptying is very fast in fasted state and that drug dissolution might mostly take place in intestinal media. Contrarily to stomach's conditions where the buffered suspension should play a role in limiting drug dissolution, no differences shall be observed between the two systems in this case. In fact, the lower extent of exposure observed in fed state for the buffered ucb-35440-3 nanosuspension (2614 ng.h/ml) compared to the un-buffered nanosuspension (3736 ng.h/ml) can be explained by a smaller dissolved amount due to the higher pH of the buffer compared to the nominal stomach pH in fed state. The GRT in both cases was thought to be the same.

When comparing the pharmacokinetic profile of both un-milled ucb-35440-3 and ucb-35440-3 nanoparticles in un-buffered media, we observe an approximate twofold decrease (7100 → 3736 ng.h/ml) in extent of exposure for the latest in fed state. This rather unexpected result could be explained by the fact that un-milled ucb-35440-3, unlike ucb-35440-3 nanoparticles, was administered as a viscous suspension (i.e. suspension homogeneity – sedimentation of large particles). This might increase the GRT of the drug and thus increase the time available for ucb-35440-3 dissolution. The arrival of the drug in dissolved state in the intestine being more progressive, chance for drug reprecipitation is smaller than for nanoparticulate formulations.

Through the data obtained, we can see that highly dosed, poorly water soluble weak base, as ucb-35440-3, represents a model with great complexity when considering nanoparticulate systems as formulation approach for systemic exposure enhancement. We could see that for basic compounds, there is an interest to increase drug solubilization in the stomach and to increase GRT. Further investigations in the eventuality of drug reprecipitation, which was only posed as an hypothesis, need to be carried out in future work.

4. Conclusions

Through this study, it has been shown that formulation of ucb-35440-3, a model poorly water-soluble weak base, as nanocrystals has met great success in regard to enhancement of drug dissolution characteristics. High pressure homogenization was shown to be a simple and adequate technique for drug particle size reduction and did not seem to alter the crystalline state of the drug, which should be highly relevant when considering drug time-stability. Pharmacokinetic evaluation of the systems clearly indicated the carefulness needed to be taken when considering poorly water-soluble drugs with pH-dependant solubility profile. Further evaluations in the in vivo behavior of the systems formed need to be carried out in order to understand phenomenon such as the eventuality of intestinal drug reprecipitation.

Acknowledgements

The authors thank UCB S.A. Pharma for the sponsorship of this work and the Industrial Chemistry Department of ULB for SEM and PXRD analysis.

References

[1] R. Löbenberg, G.L. Amidon, Modern bioavailability, bioequivalence and biopharmaceutics classification system. New scientific approaches to international regulatory standards, Eur. J. Pharm. Biopharm. 50 (2000) 3–12.
[2] N. Rasenack, H. Hartenhauer, B.W. Müller, Microcrystals for dissolution rate enhancement of poorly water-soluble drugs, Int. J. Pharm. 254 (2003) 137–145.
[3] M. Mosharraf, C. Nyström, The effect of particle size and shape on the surface specific dissolution rate of microsized practically insoluble drugs, Int. J. Pharm. 122 (1995) 35–47.
[4] Y. Wu, A. Loper, E. Landis, L. Hettrick, L. Novak, K. Lynn, C. Chen, K. Thompson, R. Higgins, U. Batra, S. Shelukar, G. Kwei, D. Storey, The role of Biopharmaceutics in the development of a clinical nanoparticle formulation of MK-0869: a Beagle dog model predicts

improved bioavailability and diminished food effect on absorption in humans, Int. J. Pharm. 285 (2004) 135–146.
[5] G.G. Liversidge, K.C. Cundy, Particle size reduction for improvement of oral bioavailability of hydrophobic drugs: I. Absolute oral bioavailability of nanocrystalline danazol in beagle dogs, Int. J. Pharm. 125 (1995) 91–97.
[6] R.H. Müller, K. Peters, Nanosuspensions for the formulation of poorly soluble drugs: I. Preparation by a size reduction technique, Int. J. Pharm. 160 (1998) 229–237.
[7] R.H. Müller, C. Jacobs, O. Kayser, Nanosuspensions as particulate drug formulations in therapy rationale for development and what we can expect for the future, Adv. Drug. Del. Rev. 47 (2001) 3–19.
[8] M.J. Grau, O. Kayser, R.H. Müller, Nanosuspensions of poorly soluble drugs – reproducibility of small scale production, Int. J. Pharm. 196 (2000) 155–157.
[9] K.P. Krause, R.H. Müller, Production and characterisation of highly concentrated nanosuspensions by high pressure homogenization, Int. J. Pharm. 214 (2001) 21–24.
[10] J. Hecq, M. Deleers, D. Fanara, H. Vranckx, K. Amighi, Preparation and characterization of nanocrystals for solubility and dissolution rate enhancement of nifedipine, Int. J. Pharm. 299 (2005) 167–177.
[11] S. Chu, S. Tanaka, J.D. Kaunitz, M.H. Montrose, Dynamic regulation of gastric surface pH by luminal pH, J. Clin. Invest. 103 (1999) 605–612.